

Proceeding Paper

Numerical Simulation of Nocturnal Ozone Increase in Metropolitan Area of São Paulo [†]

Viviana Vanesa Urbina Guerrero ¹, Marcos Vinicius Bueno de Moraes ^{2,*}, Edmilson Dias de Freitas ¹ and Leila Droprinchinski Martins ³

¹ Instituto de Astronomia, Geofísica e Ciências Atmosféricas, Universidade de São Paulo, São Paulo 05508-090, Brazil; viviana.urbina@gmail.com (V.V.U.G.); edmilson.freitas@iag.usp.br (E.D.d.F.)

² Departamento de Obras Civiles, Facultad de Ciencias de la Ingeniería, Universidad Católica del Maule, Av. San Miguel 3605, Talca 3480112, Chile

³ Department of Chemistry, Federal University of Technology—Paraná, Pioneiros Avenue, 3131, Londrina-PR 86036-370, Brazil; leilamartins@utfpr.edu.br

* Correspondence: bmarcos@ucm.cl; Tel.: +56-712-203-566

[†] Presented at the 3rd International Electronic Conference on Atmospheric Sciences, 16–30 November 2020; Available online: <https://ecas2020.sciforum.net/>.

Abstract: In large cities, pollution can not only cause deaths and illness due to exposure of people to it, but it can also reduce visibility on days of high atmospheric stability and high emission of pollutants, which can even result in vehicular accidents. Ozone is an atmospheric oxidizing gas that forms in minimal amounts naturally. People's health can be affected by the ozone present in the air they breathe, even in low concentrations, which can worsen preexisting diseases and increase hospital admissions for respiratory diseases, especially in babies, after episodes of high pollutant levels. An increase in secondary peaks during the night of this atmospheric pollutant occurs in several parts of the world, but its formation depends on the local condition. In this sense, this work aims to study the regional atmospheric characteristics for the nocturnal ozone formation in the Metropolitan Area of São Paulo (MASP). For this, the Simple Photochemical Module (SPM) coupled with the BRAMS (Brazilian Developments of Regional Atmospheric Modeling System) will be used to simulate this condition for the urban region. The results showed that the secondary nocturnal maximum of ozone concentrations in MASP is related to vertical transport of this pollutant from higher levels of the atmosphere to the surface.

Keywords: nocturnal ozone; air quality modeling; simple photochemical modeling

Citation: Urbina Guerrero, V.V.; de Moraes, M.V.B.; de Freitas, E.D.; Martins, L.D. Numerical Simulation of Nocturnal Ozone Increase in Metropolitan Area of São Paulo. *Proceedings* **2021**, *4*, 24. <https://doi.org/10.3390/ecas2020-08140>

Academic Editor: Anthony R. Lupu

Published: 13 November 2020

Publisher's Note: MDPI stays neutral with regard to jurisdictional claims in published maps and institutional affiliations.



Copyright: © 2020 by the authors. Licensee MDPI, Basel, Switzerland. This article is an open access article distributed under the terms and conditions of the Creative Commons Attribution (CC BY) license (<http://creativecommons.org/licenses/by/4.0/>).

1. Introduction

Pollutants are naturally present in the atmosphere due to fires, volcanic eruptions and biogenic emissions; however, the greatest contribution is currently associated with anthropic activities. In Latin America, urban centers are in constant development and growth, generating numerous problems associated with the effects of pollution [1]. In large cities, pollution can not only cause deaths and illness due to exposure of people to it, but it can also reduce visibility on days of high atmospheric stability and high emission of pollutants, and can even result in vehicular accidents [2–4]. Several studies have shown that the meteorological condition has a great influence on the concentrations of pollutants [5–9].

Ozone (O₃) is an atmospheric oxidizing gas that forms in very small amounts naturally. This secondary photochemical pollutant is formed in the atmosphere by photo dissociation of nitrogen dioxide (NO₂) by ultraviolet light. As it is an oxidant pollutant, ground-level ozone concentration can affect people's health (especially children, the elderly and people in outdoor activities), worsen pre-existing diseases and increase the

number of hospitalizations by respiratory diseases in risk groups [10]. Moreover, ozone exposure can be related to morbidity and mortality by cardiopulmonary diseases [11]. In the United States, ozone contributes to increasing the mortality rate associated with respiratory diseases, with an increment of 10 ppb in ground-level concentrations leading to a 3% increase in death risk associated with exposure [12]. Climatic change could be responsible for an increase in ozone concentrations and, consequently, for the number of hospital admissions and deaths associated with ozone exposure [4]. Since changes in ozone concentrations are, in part, a consequence of changes in the atmospheric system, it is important to know which synoptic patterns are associated with singular conditions of ground-level ozone concentrations.

During the night, at very stable conditions, especially under anticyclonic conditions, the increase of this contaminant has been observed with a well-defined behavior [13]. In cyclonic conditions, NO_x can occur in small amounts due to increased ventilation, and affect O₃ concentration [14]. The magnitude and frequency of nocturnal ozone peaks are generally observed in summer time, and can be associated with horizontal transport processes [15]. Additionally, in China, the nocturnal O₃ concentration is higher in suburban areas than in urban areas before it increases, reduced under the effect of vertical transport [16].

Given the importance and the elements that influence the magnitude and frequency of nocturnal ozone, this work aims to study the regional characteristics of the atmosphere of the Metropolitan Area of São Paulo in the formation of secondary ozone peaks during the night. For this, regional numerical modeling coupled with a chemical module will be used.

2. Methodology

2.1. Study Area

The Metropolitan Area of São Paulo (MASP) is located in southeastern Brazil, in a region of rugged topography (Figure 1), in which the city of São Paulo is located in the most central region coinciding with the valleys of the Tietê and Pinheiros rivers, between Serra do Mar and Serra da Cantareira, the latter with elevations above 1000 m. The MASP comprises 39 municipalities and almost half of the state's total population (approximately 20 million inhabitants) is concentrated there, covering an area of 8051 km² [17].

Given the proximity of the MASP to the coast, the surface extension of the urban area and the heat island effect seen in it make this type of thermal origin generate a significant influence on the flow patterns [18] in the dispersion of pollutants. The passage of the sea breeze creates a favorable condition for the dispersion of pollutants in this urban region, while days with extreme heat island events generate a more stable condition on the RMSP, which may favor the accumulation of pollutants [9]. In winter and early spring, there is a greater frequency of days with the influence of high-pressure systems that hinder the passage of cold fronts, favoring the formation of a high-intensity heat island, which generates more appropriate conditions for the occurrence of high pollutant concentration events [19].

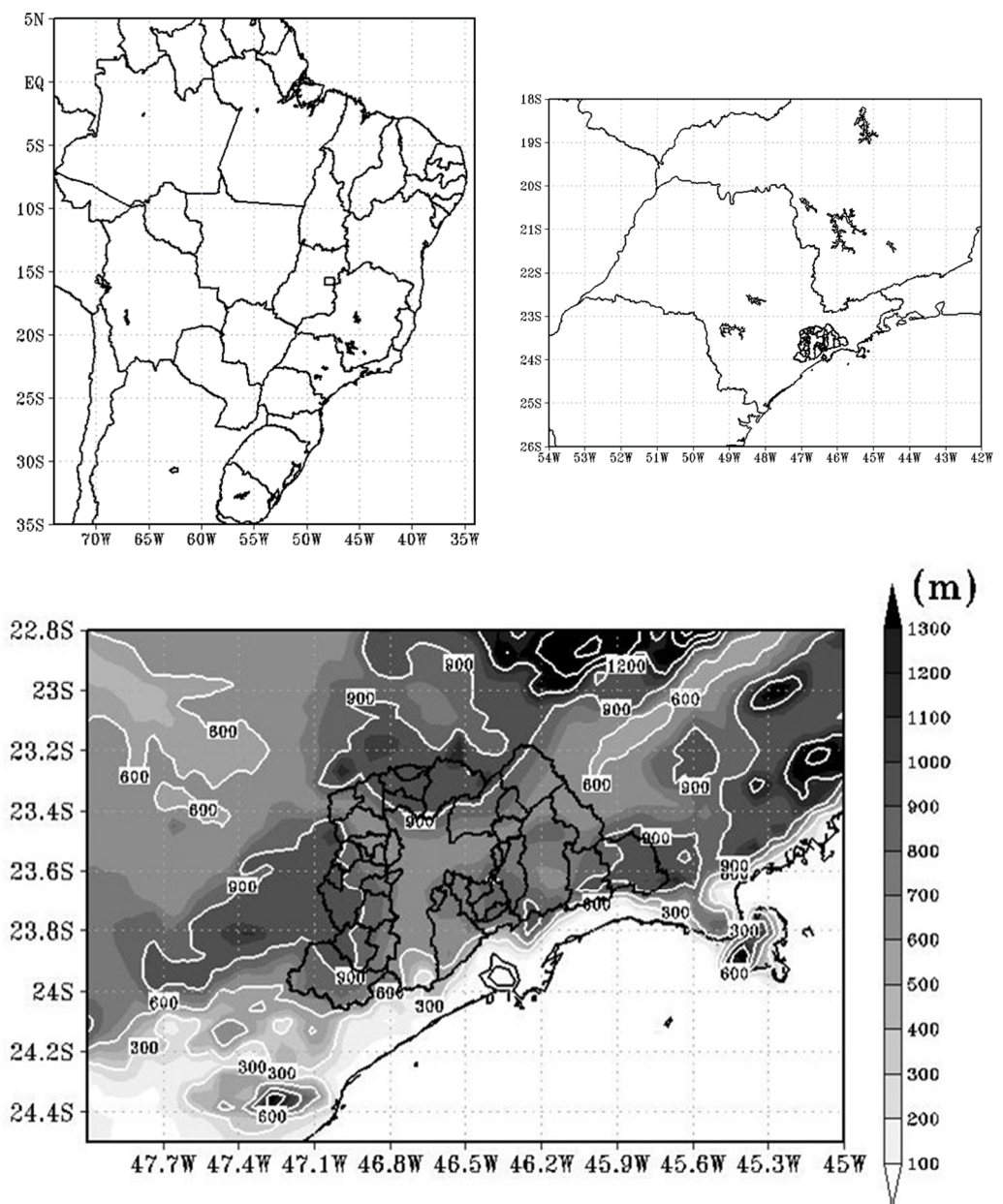


Figure 1. Location and topography map of the Metropolitan Area of São Paulo (MASP). Scale color bar in meters.

2.2. SPM-BRAMS

In this work, version 3.2 of the BRAMS model (Brazilian Development on Regional Atmospheric Modeling System, [20]) was used, which is based on the Regional Atmospheric Modeling System (RAMS, [21]). The model allows to simulate several spatial scales, integrating the microscale with the larger scales. The system of equations that governs the atmospheric state is solved using second-order finite difference schemes, both in time and space. The conservation of mass, moment, and energy in the model is guaranteed since the advection terms of these equations are treated in flow. Numerical instability is minimized by using smaller time steps in solving equations in higher resolution grids. Atmospheric physical processes not explicitly resolved by the model are parameterized. The model has a multiple grid scheme that allows the simultaneous resolution of the equations. The interaction processes between the surface and atmosphere are carried out at

BRAMS using the LEAF-3 model (Land Ecosystem–Atmosphere Feedback model version 3, [22]) for vegetated areas and with TEB (Town Energy Budget, [23]) for urban areas.

Figure 2 presents the nesting grids used in the simulations centered at MASP (-23.60° , -46.65°). The horizontal spacing grid of both domains is 16 and 4 km, from lower to the higher resolution. For the topography, files with spacing between 1 km grid points provided by the United States Geological Survey (USGS) were used. For the sea water surface temperature, weekly mean values corresponding to the simulated periods were used as input data, without considering the update of these files during the rounds. As input meteorological data, the Global Forecasting System (GFS) global model's outputs with a horizontal spacing grid of 1° were used. For all analysis of the results, the simulations were run one day before the nocturnal event, and we reject the first 24 h to avoid the spin-up effect [24] of the meteorological part of the model and to allow the model to accumulate more realistic amounts of pollutants in the atmosphere. The first level of the model output considered is 33.4 m above the surface. The model physics and land use parameterization configuration are the same as in Morais et al. [25].

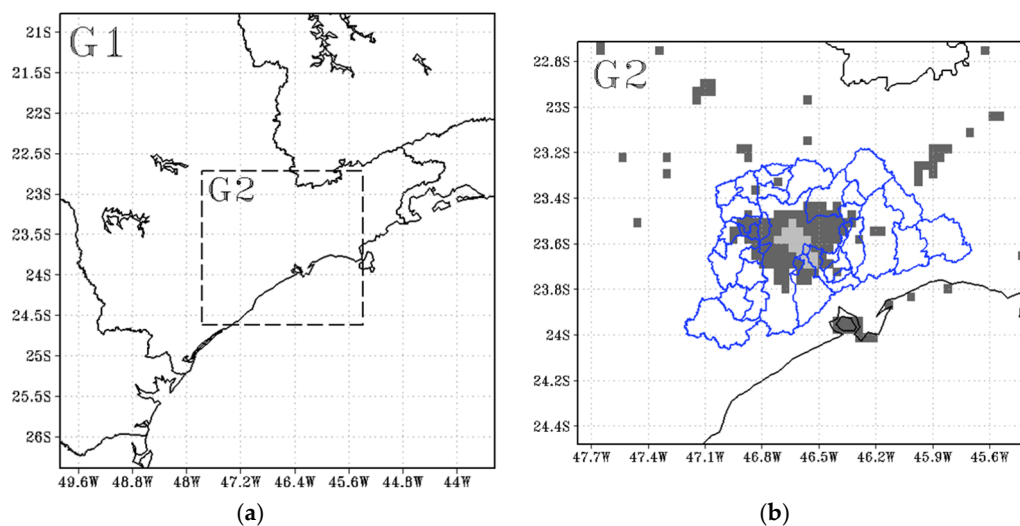


Figure 2. Grid domains used in the simulation. (a) Lower resolution domain (G1) and (b) higher resolution. Lighter gray color represents the dense urban area since dark gray is the suburban area (similar to Morais et al. [25]).

The Simple Photochemical Module (SPM, [26]) was inserted in the BRAMS model to generate operational forecasts of ozone concentrations and other constituents for the MASP with only 15 chemical reactions. Ozone formation was represented without considering hydrocarbon speciation. These equations were selected from the chemical mechanism SAPRC-99, which in turn is used in the CIT photochemical model (California Institute of Technology, [27]). Volatile organic compounds are considered in a single category to simplify the numerical scheme and reduce the calculation time. The emissions module consists of an Eulerian dispersion model integrating the mass conservation equation, which distributes the emission. For vehicular emission, the emission is still distributed in space and time within the grid following a daily cycle based on a Gaussian pair to represent the times with the highest flow vehicular. The module also makes an adjustment to consider variations in emissions during the week and on weekends. The same parameterization solves the terms of advection and turbulent transport of pollutants as the model.

2.3. Model Evaluation

In this work, two statistical indices were used to assess the proximity of the result generated by the model with the observed values of O_3 in the MASP. The bias (or mean

error) measures the model’s tendency to underestimate or overestimate the value of a variable with its observed value and is defined by the expression

$$BIAS = \frac{1}{N} \sum_{i=1}^N (S_i - O_i), \tag{1}$$

where S_i corresponds to the i th value of the simulated variable, and O_i for the same observed variable. N is the number of data.

The Root Mean Square Error (*RMSE*) is used to express the accuracy of the numerical results and is given by the following equation:

$$RMSE = \frac{1}{N} \sum_{i=1}^N \sqrt{(S_i - O_i)^2}, \tag{2}$$

where S_i corresponds to the i th value of the simulated variable, and O_i for the same observed variable. N is the number of data

Some representative points of CETESB’s (*Companhia Ambiental do Estado de São Paulo*—São Paulo state environmental sanitation technology company) pollutant monitoring stations were chosen to assess the model’s performance in representing the concentration at levels close to the surface. The locations of these points are shown in Figure 3. For meteorological variables, the model was extensively validated by Morais et al. [25,28].

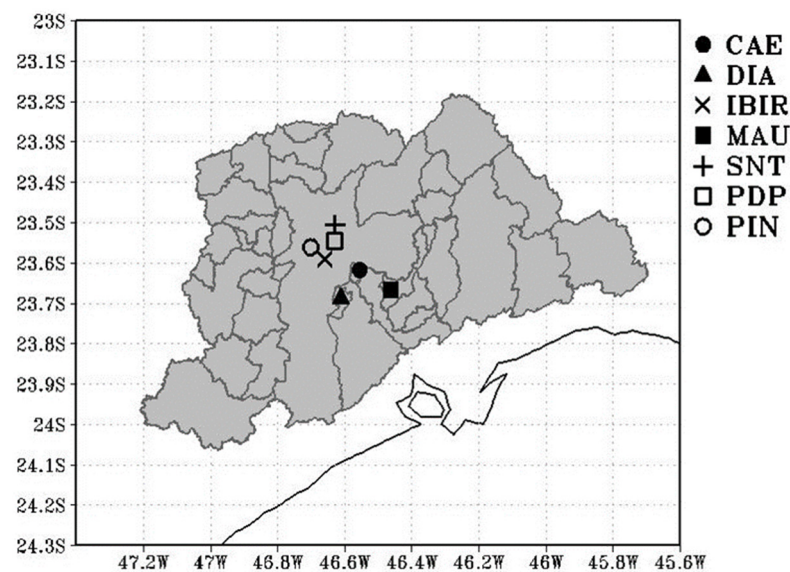


Figure 3. Location of CETESB’s monitoring network stations in the Metropolitan Region of São Paulo (in gray) used for this study, where CAE corresponds to São Caetano do Sul station, DIA to Diadema station, IBI to Parque do Ibirapuera station, MAU to Mauá station, SNT to Santana station, PDP to Parque Dom Pedro II station and PIN to Pinheiros station.

2.4. Experimental Design

Two different periods were considered to study the local meteorological factors that influence the increase in nocturnal ozone concentration. The first one corresponds to the condition where the nighttime ozone increase was recorded in all stations (case 7E), which occurred on 25 December 2010. The second was considered a period where nocturnal ozone was not recorded in any of the selected stations (case 0E). The last one was on 22 January 2005. The discussion was done by analyzing the O_3 evolution in each station and by an average nocturnal concentration map. Afterwards, a vertical profile of the ozone was created, considering the latitude of MASP.

3. Results and Discussions

3.1. Model Evaluation

Figure 4 shows a scatter plot of the RMSE and BIAS of the ozone concentration for all air quality stations in MASP. From the BIAS results, it appears that the model tends to underestimate the values of O₃. The absolute value of these indices is related to the order of magnitude of the variable. However, it appears that the values are like those obtained by other authors [6,29]. Furthermore, it is noted that the Ibirapuera park station has the worst rates, which may be related to the intense presence of green areas in the place, indicating a need to improve this type of representation in the model [28].

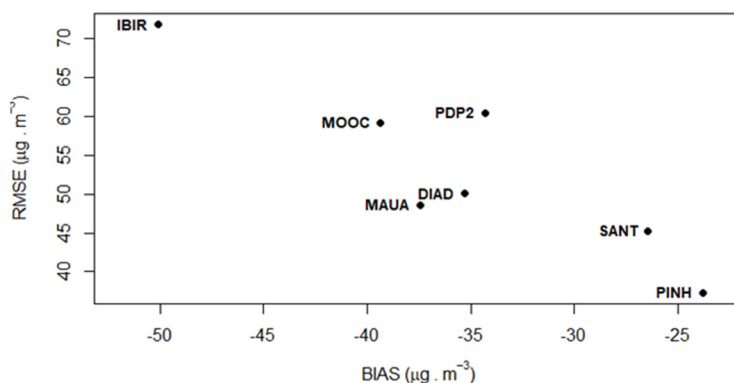
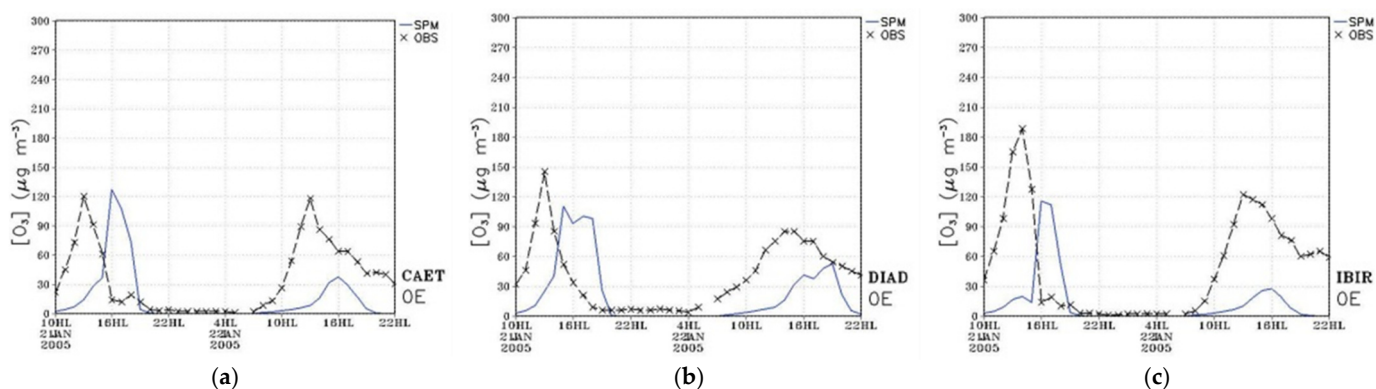


Figure 4. RMSE versus bias (or mean error) for ozone concentration. Each point represents an air quality station in the MASP: São Caetano do Sul (CAET), Diadema (DIAD), Ibirapuera Park (IBIR), Mauá (MAUA), Pq. D. Pedro II (PDP2), Pinheiros (PINH) and Santana (SANT).

3.2. Nocturnal Ozone Experiments

3.2.1. No Increase in Ozone Concentration (0E)

Figure 5 shows the concentrations simulated by the model for air quality stations in cases where no increase in ozone concentration was observed during the night (0E, left column). In the 0E case, the model represented the behavior of nocturnal concentrations relatively well, with the diurnal peak being underestimated, especially on the second day. The mean ozone field and reduced pressure at mean sea level (Figure 6) show an anticyclone located southeast of the simulation domain, which concentrates the core of maximum ozone concentration values. Values below $36 \mu\text{g} \cdot \text{m}^{-3}$ are observed in almost the entire continental part. The pressure field tends to be homogeneous over the RMSP and the average wind in this period is weak.



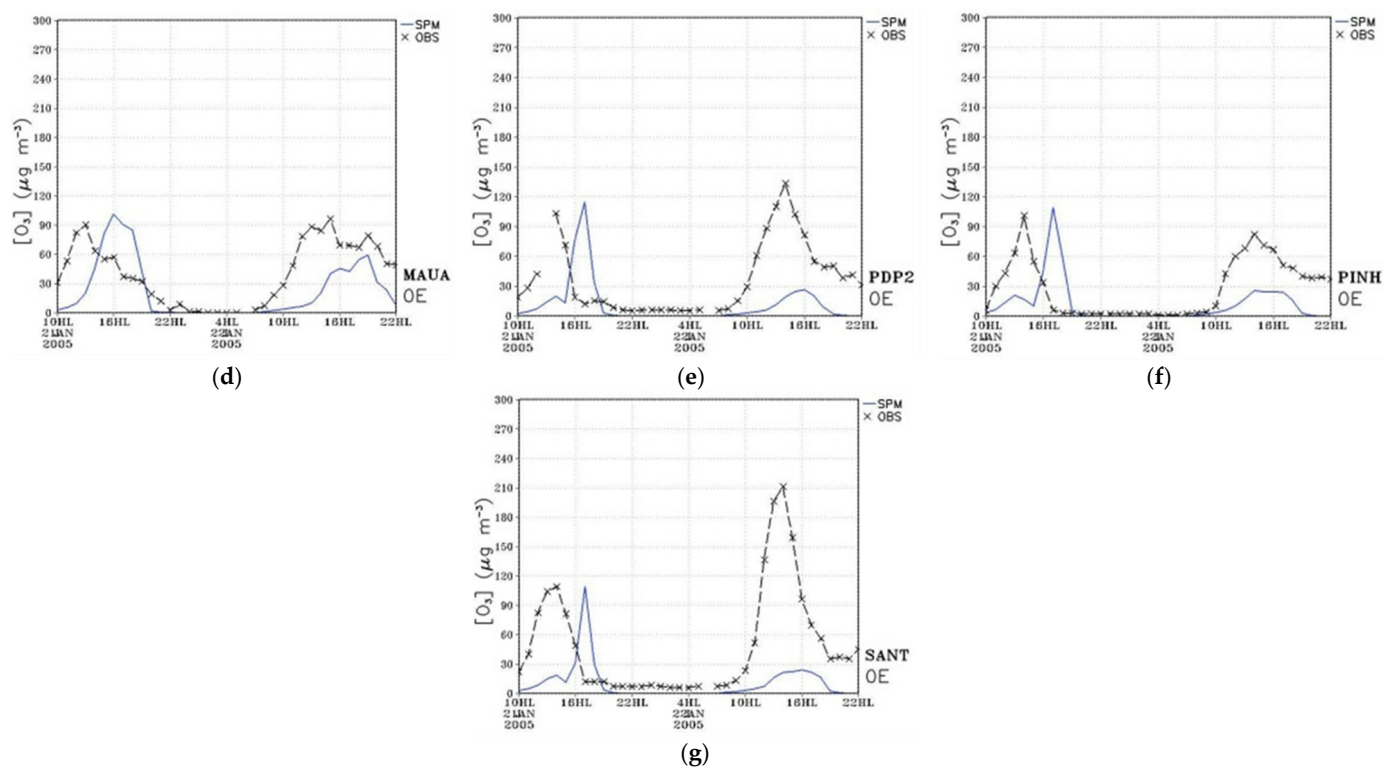


Figure 5. Ozone concentration (in $\mu\text{g m}^{-3}$) measurement observed (OBS, black-x line) and simulated (SPM, blue line) for (a) São Caetano do Sul (CAET), (b) Diadema (DIAD), (c) Ibirapuera Park (IBIR), (d) Mauá (MAUA), (e) Pq. D. Pedro II (PDP2), (f) Pinheiros (PINH) and (g) Santana (SANT).

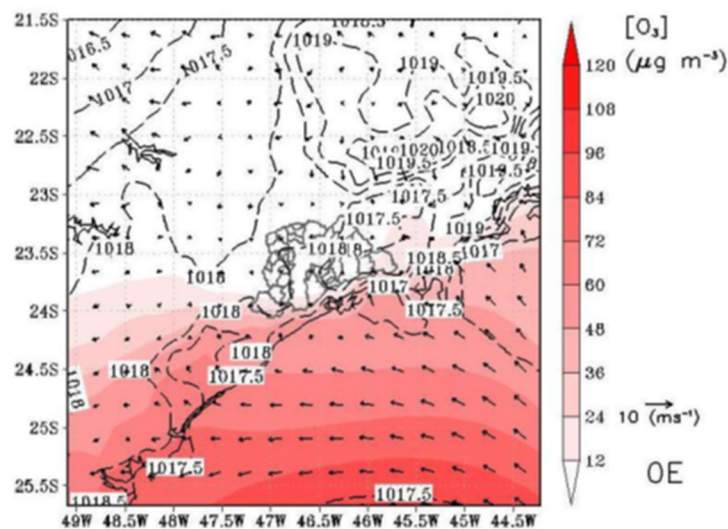


Figure 6. Average ozone concentration (color bar, in $\mu\text{g m}^{-3}$), reduced pressure at average sea level (hPa), and average wind (m s^{-1}) for the corresponding period between 22 h and 10 h (local time) at the first output level of the model.

3.2.2. Increase in Ozone Concentration (7E)

In the 7E case (Figure 7), the model represented the nocturnal increase in ozone, although, in most seasons, an underestimation occurred (difference of almost $30 \mu\text{g m}^{-3}$). At Diadema and Parque Dom Pedro II stations, although the nocturnal increase in ozone has been represented, there is a lag in the model's concentration and that obtained in such stations. Regarding daytime maximums, there was an overestimation for both days at all points analyzed. The average ozone field for this simulation (Figure 8) showed values below $24 \mu\text{g m}^{-3}$ in the continental part and a core of maximum values southwest of the

domain, where the wind tends to have a higher average intensity when compared to the rest of the study area.

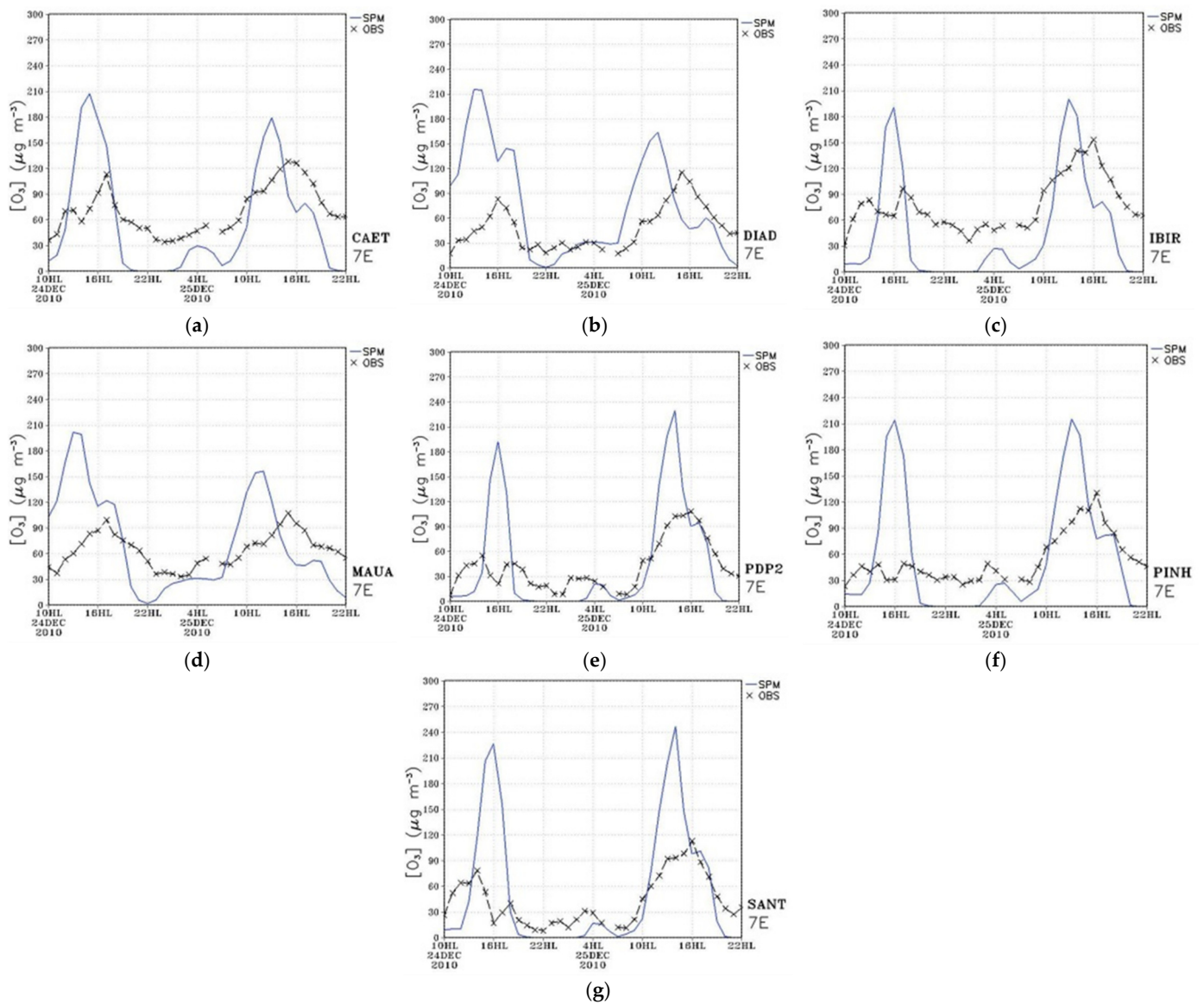


Figure 7. Ozone concentration (in $\mu\text{g m}^{-3}$) measurement (OBS, black-x line) and simulated (SPM, blue line) for (a) São Caetano do Sul (CAET), (b) Diadema (DIAD), (c) Ibirapuera Park (IBIR), (d) Mauá (MAUA), (e) Pq. D. Pedro II (PDP2), (f) Pinheiros (PINH) and (g) Santana (SANT).

3.2.3. Ozone Vertical Profile

In case 0E (Figure 9), the wind remains weak throughout the period, with a minimal vertical component. The atmosphere under the MASP is clean for all hours of the night. When an increase in the concentration of ozone is observed in all stations in the MASP (case 7E, Figure 10), the sub-wind component is more intense than when this phenomenon is observed in only a few stations. This result shows that in the cases of the nocturnal peak, the vertical transport of ozone present in the residual layer has an essential contribution in the generation of increased concentration at levels close to the surface.

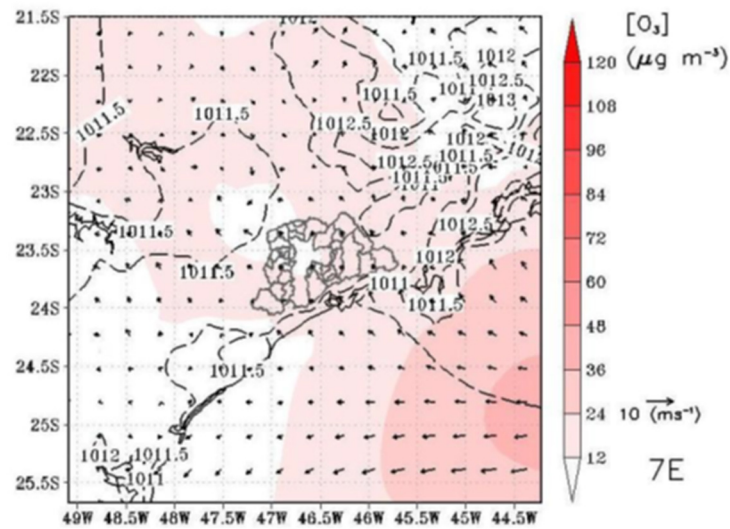


Figure 8. Average ozone concentration (color bar, in $\mu\text{g m}^{-3}$), reduced pressure at average sea level (hPa) and average wind (m s^{-1}) for the corresponding period between 22 h and 10 h (local time) at the first output level of the model.

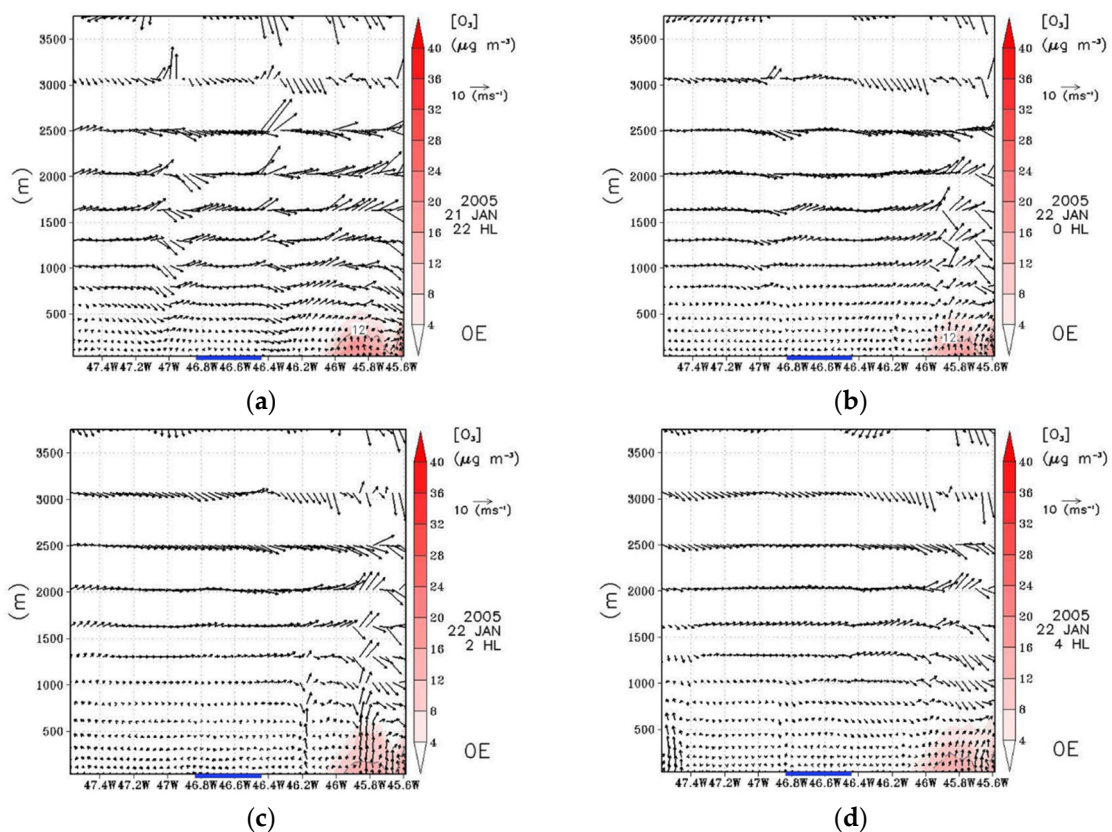


Figure 9. Ozone concentration ($\mu\text{g m}^{-3}$) and vertical wind component (m s^{-1}) with the zonal wind (m s^{-1}) for a vertical view at 23.616°S latitude, for the case 0E. The blue line indicates the location of the MASP. Local time is indicated in the corresponding figure. (a) 22 HL; (b) 0 HL; (c) 2 HL; (d) 4 HL.

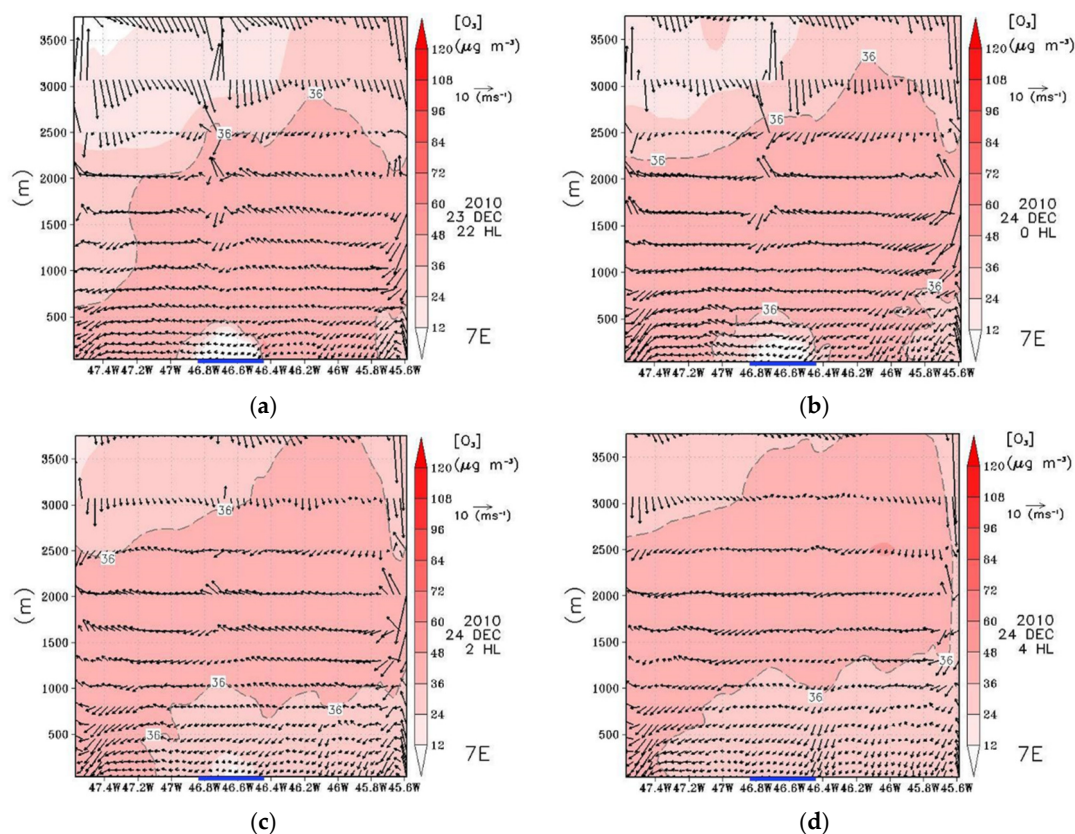


Figure 10. Ozone concentration ($\mu\text{g m}^{-3}$) and vertical wind component (m s^{-1}) with the zonal wind (m s^{-1}) for a vertical view at 23.616° S latitude, for the case 7E. The blue line indicates the location of the MASP. Local time is indicated in the corresponding figure. (a) 22 HL; (b) 0 HL; (c) 2 HL; (d) 4 HL.

4. Conclusions and Remarks

To study at a local level the characteristics that contribute to an increase in nocturnal ozone concentrations in the MASP, two cases were simulated, when no increase is observed (0E) and when the secondary peak is observed in all air quality stations (7E). Overall, the model was able to better represent the nocturnal evolution of ozone concentrations close to the surface at stations located in the MASP. For daytime concentrations, the model simulated concentrations with the maximum values overestimated. The atmospheric condition resulting from the simulations for MASP was similar, confirming that the formation of nightly ozone peaks is not linked to the synoptic situation in this study region. In this case, the greatest influence resides in the amount of ozone that is trapped in the residual layer and the intensity of the subsiding currents over the urban area, as seen in the vertical sections for all cases.

Author Contributions: All authors have contributed equally. All authors have read and agreed to the published version of the manuscript.

Funding: The authors would like to thank the financial support of the Coordenação de Aperfeiçoamento de Pessoal de Nível (CAPES) and the São Paulo Research Foundation (#2011/01040-0).

Conflicts of Interest: The authors declare no conflict of interest.

References

1. Liana, M.; Edison, O.; Jorge, M.; Marcos, M.; Leda, A.; Guerrero, U.; Leila, M.D. Current state of air quality in major cities of Latin America. *Ciência e Nat.* **2016**, *38*, 523–531, doi:10.5902/2179460X20290.
2. Patz, J.A.; Campbell-Lendrum, D.; Holloway, T.; Foley, J.A. Impact of regional climate change on human health. *Nature* **2005**, *438*, 310–317, doi:10.1038/nature04188.

3. Woodall, G.M.; Hoover, M.D.; Williams, R.; Benedict, K.; Harper, M.; Soo, J.C.; Jarabek, A.M.; Stewart, M.J.; Brown, J.S.; Hulla, J.E.; et al. Interpreting mobile and handheld air sensor readings in relation to air quality standards and health effect reference values: Tackling the challenges. *Atmosphere* **2017**, *8*, 182, doi:10.3390/atmos8100182.
4. Bell, M.L.; Zanobetti, A.; Dominici, F. Who is More Affected by Ozone Pollution? A Systematic Review and Meta-Analysis. *Am. J. Epidemiol.* **2014**, *180*, 15–28, doi:10.1093/aje/kwu115.
5. Wang, T.; Kwok, J.Y.H. Measurement and Analysis of a Multiday Photochemical Smog Episode in the Pearl River Delta of China. *J. Appl. Meteorol.* **2003**, *42*, 404–416, doi:10.1175/1520-0450(2003)042<0404:MAAOAM>2.0.CO;2.
6. Andrade, M.D.F.; Ynoue, R.Y.; Freitas, E.D.; Todesco, E.; Vara Vela, A.; Ibarra, S.; Martins, L.D.; Martins, J.A.; Carvalho, V.S.B. Air quality forecasting system for Southeastern Brazil. *Front. Environ. Sci.* **2015**, *3*, 1–14, doi:10.3389/fenvs.2015.00009.
7. Samaali, M.; Moran, M.D.; Bouchet, V.S.; Pavlovic, R.; Cousineau, S.; Sassi, M. On the influence of chemical initial and boundary conditions on annual regional air quality model simulations for North America. *Atmos. Environ.* **2009**, *43*, 4873–4885, doi:10.1016/j.ATMOSENV.2009.07.019.
8. Balzarini, A.; Pirovano, G.; Honzak, L.; Žabkar, R.; Curci, G.; Forkel, R.; Hirtl, M.; San José, R.; Tuccella, P.; Grell, G.A. WRF-Chem model sensitivity to chemical mechanisms choice in reconstructing aerosol optical properties. *Atmos. Environ.* **2015**, *115*, 604–619, doi:10.1016/j.ATMOSENV.2014.12.033.
9. Vara-Vela, A.; Andrade, M.F.; Kumar, P.; Ynoue, R.Y.; Muñoz, A.G. Impact of vehicular emissions on the formation of fine particles in the Sao Paulo Metropolitan Area: A numerical study with the WRF-Chem model. *Atmos. Chem. Phys.* **2016**, *16*, 777–797, doi:10.5194/acp-16-777-2016.
10. Romero, H.; Ihl, M.; Rivera, A.; Zalazar, P.; Azocar, P. Rapid urban growth, land-use changes and air pollution in Santiago, Chile. *Atmos. Environ.* **1999**, *33*, 4039–4047, doi:10.1016/S1352-2310(99)00145-4.
11. Mar, K.A.; Ojha, N.; Pozzer, A.; Butler, T.M. Ozone air quality simulations with WRF-Chem (v3.5.1) over Europe: Model evaluation and chemical mechanism comparison. *Geosci. Model Dev. Discuss.* **2016**, *1*, 1–50, doi:10.5194/gmd-2016-131.
12. Ren, X.; Mi, Z.; Georgopoulos, P.G. Comparison of Machine Learning and Land Use Regression for fine scale spatiotemporal estimation of ambient air pollution: Modeling ozone concentrations across the contiguous United States. *Environ. Int.* **2020**, *142*, 105827, doi:10.1016/j.envint.2020.105827.
13. Gramsch, E.; Cereceda-Balic, F.; Oyola, P.; von Baer, D. Examination of pollution trends in Santiago de Chile with cluster analysis of PM10 and Ozone data. *Atmos. Environ.* **2006**, *40*, 5464–5475, doi:10.1016/j.ATMOSENV.2006.03.062.
14. Khan, B.A.; de Freitas, C.R.; Shooter, D. Application of synoptic weather typing to an investigation of nocturnal ozone concentration at a maritime location, New Zealand. *Atmos. Environ.* **2007**, *41*, 5636–5646, doi:10.1016/j.atmosenv.2007.02.040.
15. Alp, K.; Hanedar, A.O. Determination of transport processes of nocturnal ozone in Istanbul atmosphere. *Int. J. Environ. Pollut.* **2009**, *39*, 213, doi:10.1504/IJEP.2009.028686.
16. Zhu, X.; Ma, Z.; Li, Z.; Wu, J.; Guo, H.; Yin, X.; Ma, X.; Qiao, L. Impacts of meteorological conditions on nocturnal surface ozone enhancement during the summertime in Beijing. *Atmos. Environ.* **2020**, *225*, 117368, doi:10.1016/j.atmosenv.2020.117368.
17. IBGE Censo Demográfico: Características da População—Mostra. Available online: <https://censo2010.ibge.gov.br/resultados.html> (accessed on 16 October 2020).
18. Nair, K.N.; Freitas, E.D.; Sanchez-Ccoyollo, O.R.; Silva Dias, M. a. F.; Silva Dias, P.L.; Andrade, M.F.; Massambani, O. Dynamics of urban boundary layer over São Paulo associated with mesoscale processes. *Meteorol. Atmos. Phys.* **2004**, *86*, 87–98, doi:10.1007/s00703-003-0617-7.
19. Andrade, M. de F.; Kumar, P.; de Freitas, E.D.; Ynoue, R.Y.; Martins, J.; Martins, L.D.; Nogueira, T.; Perez-Martinez, P.; de Miranda, R.M.; Albuquerque, T.; et al. Air quality in the megacity of São Paulo: Evolution over the last 30 years and future perspectives. *Atmos. Environ.* **2017**, *159*, 66–82, doi:10.1016/j.ATMOSENV.2017.03.051.
20. Freitas, S.R.; Panetta, J.; Longo, K.M.; Rodrigues, L.F.; Moreira, D.S.; Rosário, N.E.; Silva Dias, P.L.; Silva Dias, M.A.F.; Souza, E.P.; Freitas, E.D.; et al. The Brazilian developments on the Regional Atmospheric Modeling System (BRAMS 5.2): an integrated environmental model tuned for tropical areas. *Geosci. Model Dev.* **2017**, *10*, 189–222, doi:10.5194/gmd-10-189-2017.
21. Cotton, W.R.; Pielke Sr., R. a.; Walko, R.L.; Liston, G.E.; Tremback, C.J.; Jiang, H.; McAnelly, R.L.; Harrington, J.Y.; Nicholls, M.E.; Carrio, G.G.; et al. RAMS 2001: Current status and future directions. *Meteorol. Atmos. Phys.* **2003**, *82*, 5–29, doi:10.1007/s00703-001-0584-9.
22. Walko, R.L.; Band, L.E.; Baron, J.; Kittel, T.G.F.; Lammers, R.; Lee, T.J.; Ojima, D.; Pielke, R.A.; Taylor, C.; Tague, C.; et al. Coupled Atmosphere–Biophysics–Hydrology Models for Environmental Modeling. *J. Appl. Meteorol.* **2000**, *39*, 931–944, doi:10.1175/1520-0450(2000)039<0931:CABHMF>2.0.CO;2.
23. Masson, V. A physically-based scheme for the urban energy budget in atmospheric models. *Bound.-Layer Meteorol.* **2000**, *94*, 357–397.
24. Daley, R. (Ed.) *Atmospheric Data Analysis*; Cambridge University Press: Cambridge, UK, 1991.
25. Morais, M.V.B.; Freitas, E.D.; Marciotto, E.R.; Urbina Guerrero, V.V.; Martins, L.D.; Martins, J.A. Implementation of observed sky-view factor in a mesoscale model for sensitivity studies of the urban meteorology. *Sustainability* **2018**, *10*, 2183, doi:10.3390/su10072183.
26. Freitas, E.D.; Martins, L.D.; Silva Dias, P.L.; Andrade, M.F. A simple photochemical module implemented in RAMS for tropospheric ozone concentration forecast in the metropolitan area of São Paulo, Brazil: Coupling and validation. *Atmos. Environ.* **2005**, *39*, 6352–6361, doi:10.1016/j.atmosenv.2005.07.017.

-
27. Wang, L.; Zhang, Y.; Wang, K.; Zheng, B.; Zhang, Q.; Wei, W. Application of Weather Research and Forecasting Model with Chemistry (WRF/Chem) over northern China: Sensitivity study, comparative evaluation, and policy implications. *Atmos. Environ.* **2014**, doi:10.1016/j.atmosenv.2014.12.052.
 28. Morais, M.V.B. de; Freitas, E.D. de; Urbina Guerrero, V.V.; Martins, L.D. A modeling analysis of urban canopy parameterization representing the vegetation effects in the megacity of São Paulo. *Urban Clim.* **2016**, *17*, 102–115, doi:10.1016/j.UCLIM.2016.04.004.
 29. Pellegatti Franco, D.M.; Andrade, M. de F.; Ynoue, R.Y.; Ching, J. Effect of Local Climate Zone (LCZ) classification on ozone chemical transport model simulations in Sao Paulo, Brazil. *Urban Clim.* **2019**, *27*, 293–313, doi:10.1016/j.uclim.2018.12.007.